ISSN : 0974 - 7486 Volume 11 Issue 2

Materials Science

An Indian Journal

Full Paper

MSAIJ, 11(2), 2014 [74-84]

Synthesis of high crystalline ZSM-5 zeolite and M(II)(Zn, Cu & Ni)-ZSM-5 and evaluation of their adsorptive desulfurization performance

M.Khatamian*, S.Shoar, B.Divband

Inorganic Chemistry Department, Faculty of Chemistry, University of Tabriz, C.P. 51664, Tabriz, (IRAN)

E-mail : mkhatamian@yahoo.com

ABSTRACT

High crystalline ZSM-5 was synthesized by hydrothermal method using local Kaolin (Zonouz-East Azarbaijan- Iran). The effect of several parameters such as time and template type on ZSM-5 crystallization and also calcination medium were studied. The as-synthesized ZSM-5 was characterized by XRD, FT-IR, SEM, TEM and BET surface area techniques. The ratio of Si:Al of synthesized ZSM-5 was 13 with a surface area of around 300 m^2/g using TPABr as template. The Zn(II)-ZSM-5, Cu(II)-ZSM-5 and Ni(II)-ZSM-5 sorbents were prepared through liquid phase ion exchange (LPIE) method at room temperature. Cation Exchange Capacity (CEC) for this zeolite was determined with ICP-AES technique. The ion exchanged ZSM-5 zeolites were used as adsorbents for removing of fuel organosulfurs in order to reduce air pollutants. The effect of each individual adsorbent is studied by using a model fuel (2000 ppm thiophene in toluene). The efficiency of the adsorbents was determined by Gas Chromatography analysis. Π-complexation between thiophene ring and metal loaded in adsorbents is considered as removing mechanism. By increasing the cation amount in the adsorbents, the removing process improves. The Zn(II)-ZSM-5 adsorbent with the most metal loading amount showed the best performance in thiophene removing (~64%).

KEYWORDS

ZSM-5;
Crystallization;
Adsorptive desulfurization;
Ion exchanged ZSM-5.

INTRODUCTION

Zeolites are crystalline aluminosilicates with periodic arrangements of cages and channels that find extensive industrial use as catalysts, adsorbents and ion exchangers[1]. Many researches on zeolite have been focused on MFI type zeolites (i.e. Silicalite-1 and ZSM-5)[2].

ZSM-5, first made by Argauer and Landolt in 1971, is a medium pore zeolite with three-dimensional channels defined by 10-membered rings. Due to its unique channel structure, thermal stability, acidity and shape-selective property ZSM-5 has been used as sorbent and catalyst, so increasing attention has been devoted to the synthesis, the properties and applications of ZSM-5 zeolites. This molecular sieve with MFI structure is synthesized from hydrogels containing precursors of silicon and aluminum at autogenous pressure and temperature above 100°C. MFI-type zeolites are generally synthesized in the presence of organic templates. The challenge in preparing zeolites with high silica to alumina ratios (SAR), like ZSM-5 is to stabilize the void region within the zeolite framework against dissolution and transformation to denser, more stable phases. This can be achieved by addition of an organic molecule to the synthesis gel. Since the organic template strongly influences the phase that is crystallized, it is referred as a structure directing agent (SDA). A variety of templates has been reported for the synthesis of ZSM-5 zeolites, such as tetrapropylamine cations. The physicochemical properties of ZSM-5 zeolites are influenced by the compound used as template, the gel composition, the nature of the reagents and other factors[3].

Ion exchanged zeolites with some cations like Cu^+, Zn^{2+} and Ni^{2+} are promising sorbents for organosulfur removing due to their selectivity, easy usage and high performance. The sulfur level of commercial fuels and emissions from refineries is one of the main targets of current environmental regulations. Desulfurization by adsorption is based on the ability of a solid sorbent to selective adsorbing of the organosulfur compounds. There is an ongoing effort to develop new adsorbents to remove thiophene from commercial fuel via π-complexation. In the π-complexation mechanism the cations in the ion exchanged zeolites, can form the usual σ bonds with their s orbitals, and in addition, their d orbitals can back donate electron density to the antibonding π^* orbitals of the sulfur rings[4-6].

The aim of this work is to synthesize high crystalline ZSM-5 zeolite using local kaolin and investigate the effect of several parameters such as time, template type and also calcination medium on the structural characteristics of the prepared ZSM-5. In the next step, ion exchanged ZSM-5(Zn(II)-ZSM-5, Cu(II)-ZSM-5 and Ni(II)-ZSM-5) are prepared and it is expected to throw further light on the performance of ZSM-5 based adsorbents in thiophene removing as a model aromatic organosulfur that may mix with commercial fuels in refining process.

EXPERIMENTAL

Synthesis of ZSM-5 zeolite

ZSM-5 was synthesized hydrothermally. The following reagents were used for synthesis of zeolite: local kaolin (from Zonouz-Azerbaijan, Iran) as alumina source, Silicic acid (Fluka) as silica source, sodium hydroxide (Merck), concentrated sulfuric acid (Merck) and tetrapropylammonium bromide (Merck) as SDA.

Pretreatment of kaolin

Kaolin was prepared from Zonouz mine and preheated at 600-700°C. The amorphous preheated metakaolin phase was acid washed in order to reduce any possible impurities[7].

Synthesis procedure of ZSM-5 zeolite

Two solutions were prepared separately. 0.5 g sodium hydroxide, 2.01 g silicic acid, 1 ml n-propylamine and 1.01 g tetrapropylammonium bromide were added to 5 ml distilled water to get solution A. Solution B was obtained by adding 0.2193 g of metakaolin and 0.05 ml of concentrated sulfuric acid to 5 ml distilled water. Solution A was added to solution B while stirring. After the addition was completed, the gel was stirred to get a homogenous gel, and the gel was transferred to a stainless-steel autoclave with 70 mm long tube having 41 mm i.d. and 5 mm thickness. The sealed autoclave with Teflon internal vessel was heated at autogenous pressure in an air oven maintained at 433 K for two periods (44 and 50 hours).

Pretreatment of ZSM-5 zeolite

Calcination of zeolite was performed in order to remove the template from the as-synthesized samples.

The zeolites were calcined to 773°C in increments of 50 to 100°C, with 4°C/min temperature ramp and then in 100 to 500 °C with 10 °C/min temperature ramp. Calcination was carried out in air in an electric furnace; model PCD Shinba from Exciton Company; and also in the presence of N_2 in a horizontal 808P Carbolite furnace.

Characterization of zeolites

The prepared MFI zeolites were characterized for their chemical composition, crystallinity, surface behavior and morphology. The determination of aluminum and silicon contents in zeolite samples was carried out using standard inductively coupled plasma (ICP) method. The samples for ICP analysis were prepared by fusing the zeolite with sodium hydroxide.

The FT-IR spectra were recorded using BRUKER

Model Tensor 27 Infrared Spectrophotometer in the range 4000–400 cm^{-1} on thin wafers of KBr in which 1% (w/w) of zeolite was dispersed. Crystallinity was checked using a Siemens D500 X-ray diffractometer equipped with a Cu fine focus X-ray tube working at a generator potential of 40 kV. The zeolite samples were also characterized by scanning electron microscopy using a Leo scanning microscope model 440i. The samples in the powdered form were dried at 453K overnight and then mounted on aluminum disks. In this process, a thin layer of sample powder was spread and deposited on each aluminum disk having carbon pads. These samples were then evacuated, and then immediately coated with gold. The gold coated disks were then mounted in the sample holder of the instrument. Surface area and pore structure were measured using fully automated ASAP 2010 equipment (Micromeritics, USA). The zeolite samples were heated overnight in an oven at 473K in order to remove moisture. A weighed quantity of dry zeolite sample was degassed overnight at 573K under a vacuum of 3 mmHg. The sample was allowed to cool, reweighed and connected to the analysis port as quickly as possible in order to avoid any readsorption of moisture. At the analysis port, nitrogen was fed into the tube and adsorption of the gas took place. This was followed by desorption of nitrogen and then calculation of the surface area and other parameters.

Selective adsorption evaluation of ZSM-5 zeolite in thiophene removing

Sorbent preparation

The powder form ZSM-5 was modified by liquid phase ion exchange (LPIE), using different cations. Cu(II)-ZSM-5, Ni(II)-ZSM-5 and Zn(II)-ZSM-5 were prepared by 72 h ion exchanging ZSM-5 with saturated solutions of Cu^{2+}, Ni^{2+} and Zn^{2+} acetate salts at ambient temperature. After the exchange, the zeolite suspension was filtered and washed with copious amounts of deionized water.

Sorbent activation

All of the ion exchanged sorbents were activated at 120°C for 2 h in the presence of N_2 in order to remove the moisture and open the framework pores for better adsorption. Auto reduction of Cu(II)-ZSM-5 to Cu(I)-ZSM-5 was carried out in He at 450°C for 6 h[8,9].

Adsorption set-up

All adsorption experiments were performed with down-flow in a vertical custom-made quartz tube equipped with a supporting packed glass filter. After in situ activation of the adsorbent, a model sulfur containing solution (2000 ppm thiophene in toluene) was allowed to contact the bed and the effluent thiophene concentration was monitored as a function of passing times. Effluent samples collected during the experiments were analyzed using a Shimadzu GC-2010 unit equipped with a CP-20 capillary column and flame ionization detector (FID). All of the adsorption experiments were carried out at ambient temperature and atmospheric pressure.

RESULTS AND DISCUSSION

Characterization of synthesized zeolite

Si/Al ratio

Different alumina sources like aluminum hydroxide, aluminum sulfate, etc. have been used in literature[1,10,11], in order to ZSM-5 synthesis. In this work local kaolin with high Si amount and 18.44% Al_2O_3, was used as alumina source. Complete chemical analysis of Zonouz kaolin can be found elsewhere[7]. The Si/Al ratio is an important factor in ZSM-5 synthesis. The crystal size of the ZSM-5 zeolite decreases with increasing the SiO_2/Al_2O_3[12-14]. In this work, the SiO_2/Al_2O_3 ratio was selected 39 in the initial gel composition. After crystallization, this ratio decreases remarkably to about 13, because of the alkaline nature medium (pH=10-11) of the gel. Alkalinity leads to dissolve more and more silica in the liquid phase and therefore, less silica becomes incorporated into the crystalline solid phase; so a considerable decrease in the Si/Al ratio takes place after crystallization.

X-ray diffraction studies

Figure 1 shows the X-ray diffraction patterns of ZSM-5 zeolite powder synthesized at 160°C using tetrapropylammonium bromide as SDA for two series of crystallization time (44 and 50 h). We tried to synthesize ZSM-5 zeolite in shorter time comparing to previous works[15]. The results showed that crystallization is complete in less than 2 days. Increasing the crystallization time to 50 h not only does not lead to better crystallization, but also causes to decompose the ZSM-5 crystallized phase. In the XRD pattern of ZSM-5(50) peaks at $2\theta = 7\text{-}9°$ have been omitted. The XRD pattern for ZSM-5(44) shows peaks at $2\theta = 7\text{-}9°$ and 23-25°, which correspond to the specific peaks of ZSM-5 zeolite[1]. No other peak could be observed other than ASTM data, indicating the high purity of product. The relative crystallinity of ZSM-5 was calculated based on the intensity of the peaks of angel $2\theta = 22\text{-}25°$[3]. Average crystal size measured about 21 nm for ZSM-5(44) by Scherer's equation ($D= K\lambda 57.32 / \beta\cos\theta$) from XRD peaks between $2\theta = 7\text{-}9°$.

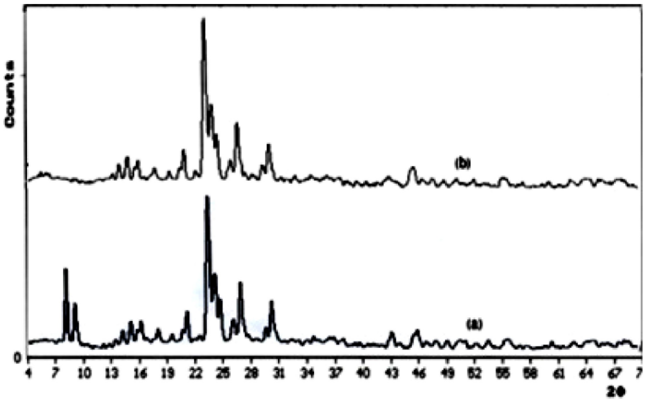

Figure 1 : XRD patterns of ZSM-5(TPABr) for (a) 44 h and (b) 50 h crystallization time

In order to investigate how calcination in the presence of N_2 effects the crystal phase of the ZSM-5, ZSM-5 was calcined both in the air and in the presence of N_2 (ZSM-5(air) and ZSM-5(N_2) respectively). Figure 2 shows the X-ray diffraction patterns of as-synthesized ZSM-5 zeolite powder synthesized at 160°C using tetrapropylammonium bromide as SDA for ZSM-5(air) and ZSM-5(N_2). In ZSM-5(N_2) the relative intensity of the peaks of angel $2\theta = 22\text{-}25°$ is higher than peaks of angel $2\theta = 7\text{-}9°$, while in ZSM-5(air), peaks of angel $2\theta = 7\text{-}9°$ has higher intensity. This results show the crystal structure difference between ZSM-5(air) and ZSM-5(N_2); thus respectively monoclinic ($P12_1/n1$ space group) and orthorhombic (*Pnma* space group) symmetry can be suggested[16].

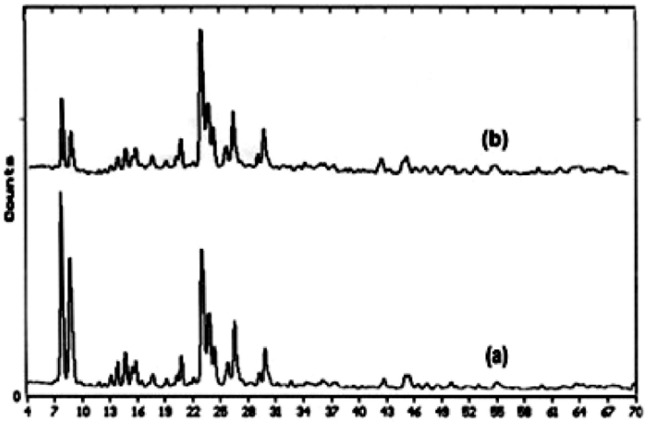

Figure 2 : XRD patterns of (a) ZSM-5(air) and (b) ZSM-5(N_2)

Different templates have been used in literature for ZSM-5 synthesis[3]. Figure 3 shows X-ray diffraction patterns of ZSM-5 zeolite powder synthesized at 160°C using tetrapropylammonium bromide (TPABr), tetrapropylammonium hydroxide (TPAOH) and ethanol-ammonia (Et-Am) as SDA. Crystallization with both TPABr and TPAOH is acceptable; however, a better crystallinity is achieved by TPABr considering the relative intensity of the peaks of angel $2\theta = 22\text{-}25°$[17]. Using Et-Am as template does not lead to ZSM-5 synthesis.

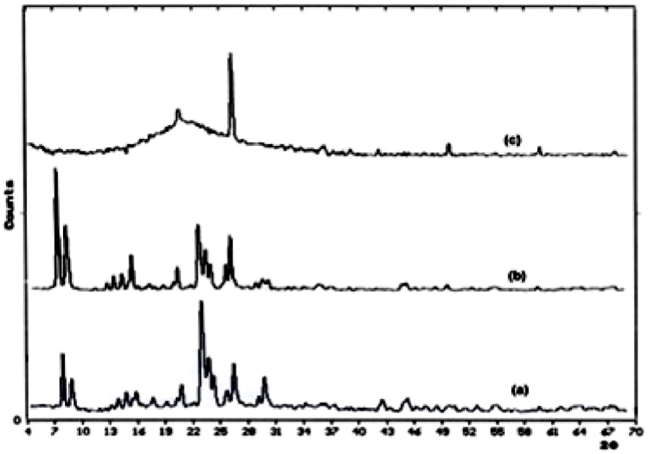

Figure 3 : XRD patterns of (a) ZSM-5(TPABr), (b) ZSM-5(TPAOH) and (c) ZSM-5(Et-Am)

Fourier transform infrared spectroscopy

The FT-IR spectra of the synthesized zeolites were recorded in the range 4000–400 cm^{-1}. Figure 4 shows the infrared spectra of ZSM-5 zeolite synthesized at 160°C using tetrapropylammonium bromide as SDA for both ZSM-5(air) and ZSM-5(N_2). Bands around 791, 1080 and 1219 cm^{-1} are characteristic of SiO_4 tetrahedron units[18]. Absorptions at 1219 and 542 cm^{-1} provide information on the differences between these zeolites and other zeolite types. The external asymmetric stretching vibration near 1219 cm^{-1} is due to the presence of structures containing four chains of five-membered rings arranged around a two-fold screw axis, as in the case of ZSM-5 structure[19]. The absorption band around 1080 cm^{-1} is attributed to the internal asymmetric stretching vibration of Si–O–T linkage of zeolite ZSM-5. The absorption near 790 cm^{-1} is assigned to the symmetric stretching of the external linkages, and the one near 542 cm^{-1} is attributed to a structure-sensitive vibration caused by the double five-membered rings of the external linkages. The absorption band near 450 cm^{-1} is due to the T–O bending vibrations of the SiO_4 and AlO_4 internal tetrahedra. The presence of absorption bands around 542 and 450 cm^{-1} are characteristic of the ZSM-5 crystalline structure[20] and the ratio of the intensities of these two peaks provides an approximate estimate of the degree of crystallinity of a given zeolite sample. These values compare to a literature value of 0.8 suggested for pure ZSM-5 zeolites, indicating that both as-synthesized zeolites also exhibit good crystallinity. In the FT-IR spectra of ZSM-5(N_2) the intensity of peaks at 450 cm^{-1} and 550 cm^{-1} is nearly identical which shows complete crystallization of the product. The Findings emerge that the bands near 1080 cm^{-1} (Internal asymmetric stretch), 790cm^{-1}(external symmetric stretch), 542cm^{-1} (double ring vibration) and 450cm^{-1} (T-O bend) were presented for two samples, due to formation of only ZSM-5 phase.

Figure 5 shows the FT-IR spectra of synthesized ZSM-5 samples using different templates. The spectra show the appearance, intensity lowering and disappearance of by using different templates.

In the case of TPABr and TPAOH, this band has grown better while in tetrabutylammonium hydroxid (TBAOH) the intensity of the band is lowered considerably. Using Et-Am as template cause to disappearing 542 cm^{-1} band, so no ZSM-5 phase is existed in the sample.

Considering the data coming from FT-IR and XRD results, tetrapropylammonium bromide was selected as the optimum template.

Scanning electron microscopy

The scanning electron micrograph of ZSM-5(TPABr) is shown in Figure 6 and shows that this zeolite is crystallized in spherical to cubical shape crystals. No amorphous phase is observable, indicating high purity of the sample.

Transmission electron microscopy

As shown in the TEM image depicted in Figure 7 (a), the ZSM-5 sample prepared with TPABr, is formed by small crystallites, with size as low as 20-30 nm. These crystals are not present as isolated particles, but they are primary particles which tend to be aggregated into secondary particles with size around 2000 nm. The well developed secondary particles (Figure 7 (b)) show quasi-spherical morphology which confirms good crystallinity of the sample under the mentioned condition. Selected area electron diffraction (SAED) reconfirms that these as-prepared secondary particles are in single crystal form.

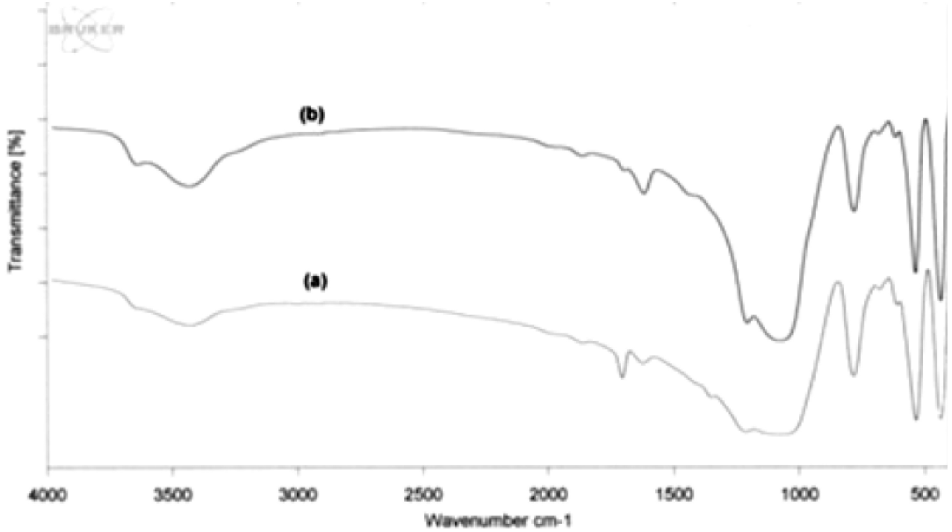

Figure 4 : FT-IR spectra of (a) ZSM-5(N_2) and (b) ZSM-5(air)

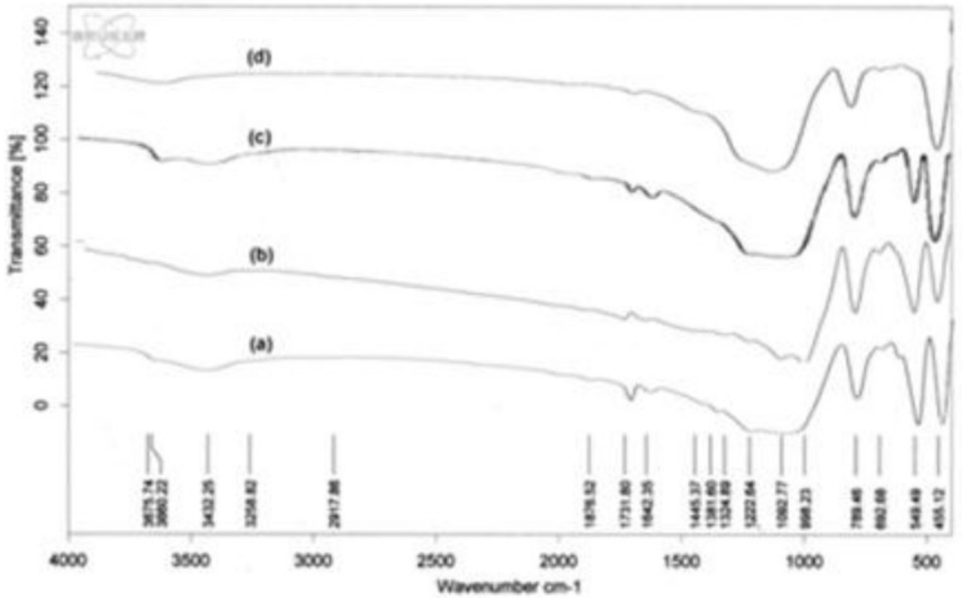

Figure 5 : FT-IR spectra of (a) ZSM-5(TPABr), (b) ZSM-5(TPAOH), (c) ZSM-5(TBAOH) and (d) ZSM-5(Et-Am)

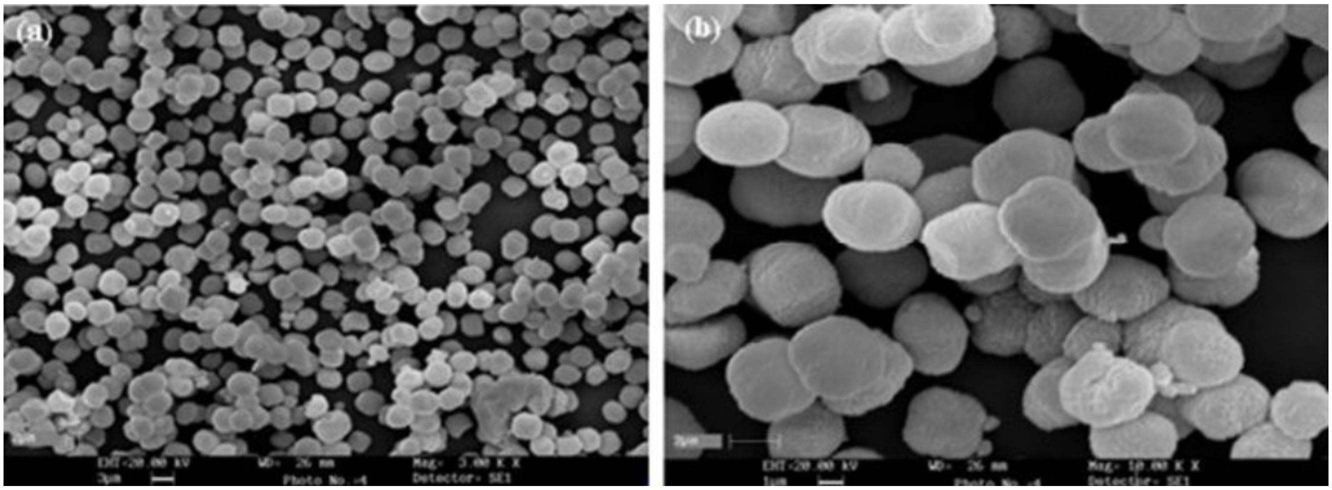

Figure 6 : SEM micrographs of ZSM-5(TPABr) (a) × 3000 and (b) × 10000 magnifications

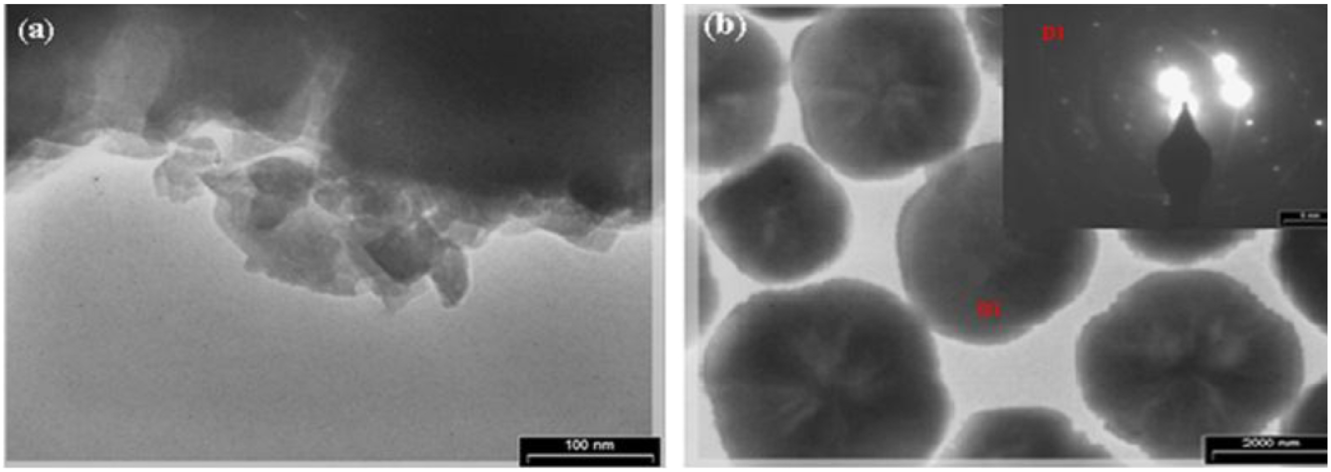

Figure 7 : TEM images of ZSM-5(TPABr) (a) small crystallites and (b) secondary particles along with selected area electron diffraction (SAED)

Surface area and pore structure determination

Figure 8 illustrates the N_2 adsorption isotherm at 76.46 K for the synthesized ZSM-5(TPABr) zeolite. The adsorption at low relative pressures corresponds with the micropore filling[21]. However, this curve cannot be classified simply as type I isotherms, which are typical of purely microporous solids. A very important adsorption is observed at high relative pressures, which originates from the nitrogen adsorption in the interparticle voids. Likewise a significant adsorption takes place at intermediate relative pressure due to the N_2 adsorption on the external zeolite surface. The sample presents external surface with value up to108 m^2/g which is in agreement with being formed by small crystallites. Another remarkable fact is the lower t-plot micropore volume and micropore surface of the sample compared with the values corresponding to micrometer size ZSM-5 sample (0.18 cm^3/g and 400 m^2/g, respectively). J. Aguado et al.[21] developed a mathematical model that correlates variation of the ZSM-5 textural properties with changes in the crystal size. This model introduces the concept of surface enhancement and crystal aggregation factors to explain the increase in both the external and the overall zeolite surface as the crystal size is reduced. Considering this model the total surface area, that would be comparable with the BET surface area, can be determined as the sum of both internal and external contributions:

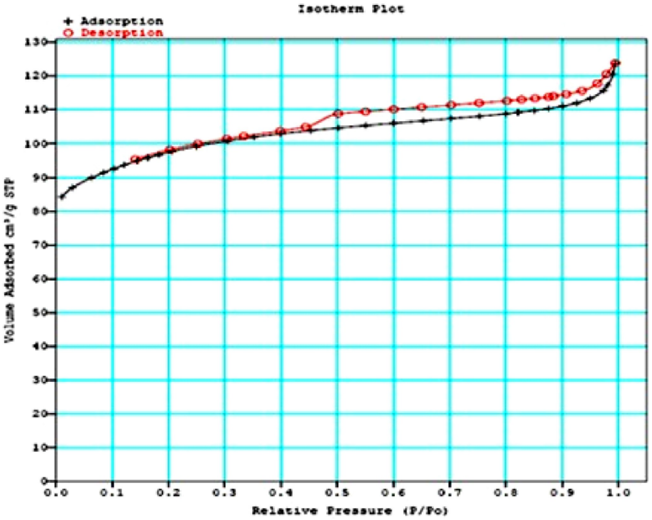

Figure 8 : N_2 adsorption isotherm at 76.46 K ZSM-5(TPABr)

$$S_{TOT}\,(m^2/g) = S_{EXT}\,(m^2/g) + S_{MIC}\,(m^2/g)$$

$$S_{TOT} = 108.13 + 164.71 = 272.84\ (m^2/g)$$

TABLE 1 summarizes the complete results of surface area determinations for synthesized ZSM-5(TPABr). Pore volume and pore size information are collected in TABLE 2.

TABLE 1 : Surface area information of synthesized ZSM-5(TPABr)

Single point surface area at P/P*= 0.30520395	304.9361 m^2/g
BET surface Area	272.8425 m^2/g
Langmuir surface Area	442.7763 m^2/g
BJH Adsorption Cumulative Pore area of pores between 17 and 3000 A Diameter	65.1914 m^2/g
BJH Desorption Cumulative Pore area of pores between 17 and 3000 A Diameter	74.8532 m^2/g
Micropore Area	164.7128 m^2/g
External surface Area	108.1297 m^2/g

TABLE 2 : Pore information of synthesized ZSM-5(TPABr)

Single point total pore volume of pores less than 742.9814 A at P/P*= 0.97324272?	0.178983 cm^3/g
BJH Adsorption Cumulative Pore Volume of pores between 17 and 3000 A Diameter?	0.07 cm^3/g
BJH Desorption Cumulative Pore area of pores between 17 and 3000 A Diameter	0.073571 cm^3/g
Micropore volume	0.103311 cm^3/g
Average pore Diameter (BET)	26.2397 Å
BJH Adsorption Average pore Diameter	43.3283 Å
BJH Desorption Average pore Diameter	39.4780 Å

ZSM-5 zeolite performance in thiophene removing

Sorbent prepration and structural properties of ion exchanged zeolite

The sorbents used in the present paper were prepared by using liquid phase ion exchange (LPIE) technique. LPIE is usually limited by the (a) selectivity of the zeolite for the new cationic species have been introduced into the framework; (b) passage of solvated cations through the zeolite apertures; (c) hydrolysis of cation species in the aqueous solution[22]. Many research groups have studied a great deal about cation exchange equilibrium and the results are very well documented in the literature[23]. In order to guarantee the maximum ion exchanged capacity, it is desired to use excess loadings and/or increase the temperature during the exchange process. However, for a particular zeolite and cation species combination, increasing the exchange process temperature could lead to collapsing of the zeolitic framework[24]. Thus all of the ion exchange processes in this work were carried out at ambient temperature but using high concentration of cation solutions (saturated solutions). In order to lessen the hydrolysis of cation species in the aqueous solutions, the solution pH was kept about 6 during the exchange process. In general, a lower pH value diminishes the occurrence of hydrolysis species.

The cation exchange capacity (CEC) of synthesized ZSM-5 (TPABr) zeolite for Cu^{2+}, Ni^{2+} and Zn^{2+} cation species, determined by ICP analyses, are summarized in TABLE 3. The selectivity of synthesized ZSM-5(TPABr) zeolite for these cation species is as follow: $Zn^{2+} > Cu^{2+} > Ni^{2+}$

The ion exchange capacity depends on a number of factors such as cation size and oxidation state, level of hydration of the zeolite, Si/Al ratio of the framework[24]. These factors determine the location of the cations and also the extent and kinetics of the ion exchange. Thus, the higher ion exchange capacity of Zn(II)-ZSM-5 as compared to Ni(II)-ZSM-5 could be due to an effective interaction of Zn^{2+} ion with zeolite framework as compared to the interaction of Ni^{2+}. The hydrated Ni^{2+} ions remain strongly coordinated to water molecules while within the zeolite pore structure[25].

According to the studies on the metal ion exchanges in zeolites, most of the transition metal ions introduced by ion exchange at room temperature are hydrated inside the cages. Upon drying and calcinations, the ions migrate to various ion exchange sites[24].

Powder X-ray diffraction (XRD) patterns of ion exchanged zeolites after drying have been collected in Figure 9, in order to investigate if the zeolite structure is retained after exchange process. The similarity in the XRD patterns, especially in the 2θ ranges 7-9° and 23-25°, between ZSM-5 zeolite and ion exchanged ZSM-5 zeolites implies that the original zeolite structure is retained. However, a small shift as well as a little intensity reduction takes place in the XRD patterns of ion exchanged zeolites which is more observable in Zn(II)-ZSM-5 sample. High Zn^{2+} loading amount leads to this slight difference in the XRD pattern of Zn(II)-ZSM-5 comparing to pure ZSM-5. Considering the CEC amounts, Cu^{2+} ions have still relatively high loading amounts (63.5 mg/g zeolite), however, the XRD pattern of Cu(II)-ZSM-5 shows little difference comparing to pure ZSM-5. It seems that the cationic sites of Cu^{2+} in the as-prepared ZSM-5 framework are probably far from interplane distances which are reflected in the XRD pattern (011, 200, 051, 033, and 313 crystal planes), so the loading of Cu^{2+} cation species in theses cationic sites cause to just negligible difference in the interplane distance (d) values.

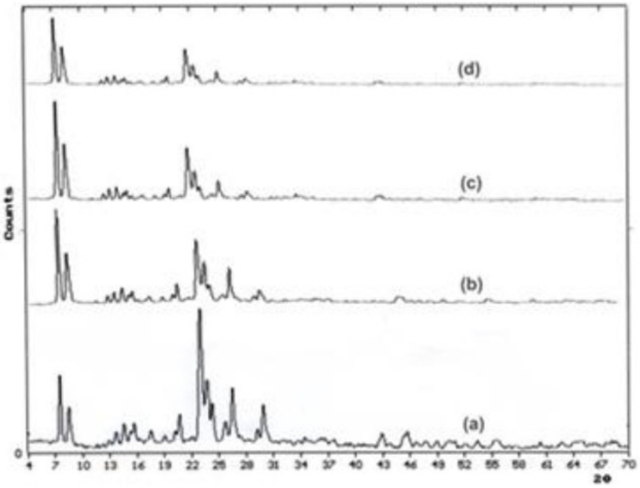

Figure 9 : XRD patterns of (a) pure ZSM-5, (b) Ni-ZSM-5, (c) Zn-ZSM-5 and (d) Cu-ZSM-5

In order to perform more investigation on the effect of ion exchange process on ZSM-5 structure, the FT-IR spectra of both Zn(II)-ZSM-5 (having the highest CEC amount) and pure ZSM-5 are given in Figure 10 No remarkable difference in the main structure sensitive peaks (542 and 1219 cm^{-1}) is observable, indicating that the ZSM-5 structural phase remained intact even after high cation loading amounts.

Sorbent activation

As mentioned in section 2, all the sorbents were carefully activated in situ, to avoid any exposure to moisture. For Cu-zeolites, this is critical since Cu^{+} species are highly unstable. Cuprous ions are known to disproportionate in the presence of water as follow[26-27]:

$$2Cu^{+} \leftrightarrow Cu^{2+} + Cu^{0}$$

Another problem that needs to be avoided during activation of the copper zeolites is the possibility of fast re-oxidation. Turnes Palomino et al.[28] and Llabre's i Xamena et al.[29] studied the re-oxidation of auto-re-

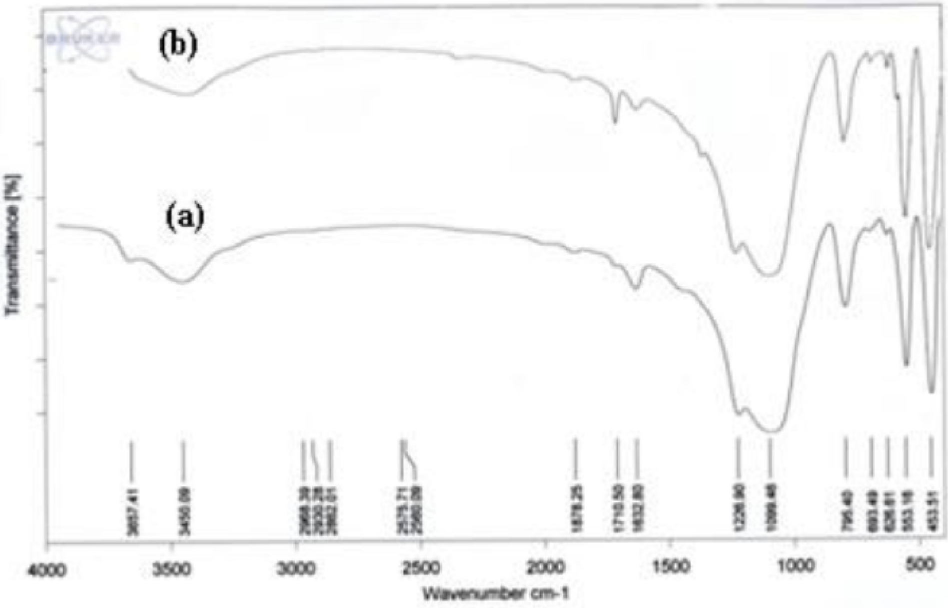

Figure 10 : FT-IR spectra of (a) pure ZSM-5, (b) Zn-ZSM-5

duced copper exchanged ZSM-5 and Mordenite zeolites, using electron paramagnetic resonance (EPR) and X-ray absorption near edge structure (XANES) analyses. In both works it was determined that the Cu^+ ions became oxidized in the presence of water or oxygen molecules and that the process was accelerated in the simultaneous presence of both oxidative species. These results reinforced the need for proper activation of ZSM-5 to maintain the maximum possible amount of cuprous ions before desulfurization tests.

Adsorptive desulfurization

After activation of the adsorbent bed, a 20 ml sample of model solution (2000 ppm thiophene in toluene) was allowed to contact the beds (containing 0.1 g of each adsorbent) and the effluent total thiophene content was monitored periodically. Breakthrough adsorption curves were generated by plotting the thiophene removing percent versus the passing times. Figure 11 shows the resulting breakthrough curves for the Zn(II)-ZSM-5, Cu(I)-ZSM-5 and Ni(II)-ZSM-5 beds. These sorbents are capable of removing more than half of thiophene content from model solution, only after 10 times passing. Among the adsorbents tested, the Zn-exchanged ZSM-5(TPABr) zeolite exhibited better performance adsorbing about 64% of thiophene content after 10 times passing of solution through the Zn(II)-ZSM-5 bed. The adsorption data infer that the adsorption efficiency is enhanced upon increasing the metal loading. Thus, the cation species loaded on the ZSM-5 zeolite are responsible for desulfurization of thiophene. This fact is in agreement with metal-thiophene ring bonding during adsorptive desulfurization process.

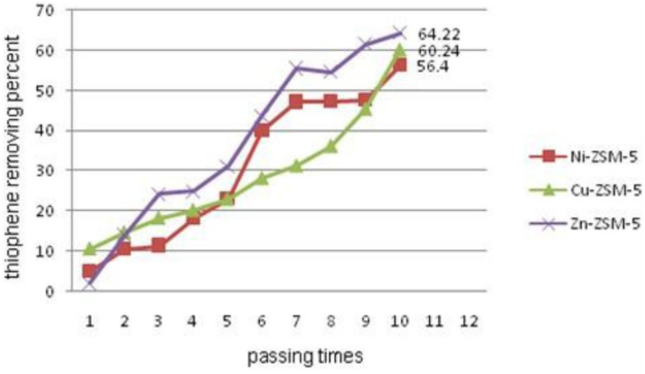

Figure 11 : Breakthrough adsorptive thiophene removing curves of Zn(II)-ZSM-5, Cu(I)-ZSM-5 and Ni(II)-ZSM-5 adsorbents

The concentration of effluent total thiophene content (ppm) collected in TABLE 4 was calculated on the basis of calibration curve (R^2=0.9999).

CONCLUSIONS

A highly crystalline ZSM-5 zeolite was synthesized from amorphous metakaolin prepared by hydrochloric acid leaching of a kaolin mineral from Zonouz mine, Iran. The syntheses were conducted with variations in the crystallization time, template type and calcination condition. Optimum condition was obtained at 160°C for 44 h, using tetrapropylammonium bromide as SDA, followed by calcinations at 500°C in the presence of N_2. The as-synthesized ZSM-5 zeolite presents crystal size in the range 20-30 nm, that tend to form larger aggregates with a size around 2000 nm. The ZSM-5 sample presents high surface area, with value up to 300 m^2/g. The average pore size of the sample is in mesoporous range. In the next process Ni(II)-ZSM-5, Zn(II)-ZSM-5 and Cu(II)-ZSM-5 adsorbents prepared by LPIE method used for thiophene adsorption. All of the sorbents were capable of removing more than half of thiophene content from model solution, only after 10 times passing. The thiophene removing process is improving as follow by increasing the metal loading amounts in ZSM-5 zeolite:

Zn(II)-ZSM-5 > Cu(I)-ZSM-5 > Ni(II)-ZSM-5

NOMENCLATURE

SAR : silica to alumia ratio
SDA : structure directing agent
LPIE : liquid phase ion exchange
Cu(II) ZSM-5 : as-synthesized ZSM-5 zeolite ion exchanged with Cu^{2+} cation species
Ni(II)-ZSM-5 : as-synthesized ZSM-5 zeolite ion ex changed with Ni^{2+} cations species
Zn(II)-ZSM-5 : as-synthesized ZSM-5 zeolite ion exchanged with Zn^{2+} cation species
Cu(I)-ZSM-5 : auto-reduced Cu(II)-ZSM-5 after activation
ZSM-5(50) : as-synthesized ZSM-5 zeolite with 50 h crystallization time
ZSM-5(44) : as-synthesized ZSM-5 zeolite with 44 h crystallization time
ZSM-5(air) : as-synthesized ZSM-5 zeolite calcined in air
ZSM-5(N_2) : as-synthesized ZSM-5 zeolite calcined in the presence of N_2
ZSM-5(TPABr) : as-synthesized ZSM-5 zeolite using tetrapropylammonium bromide as SDA
SAED : selected area electron diffraction
CEC : cation exchange capacity

ACKNOWLEDGMENTS

The supports from council of University of Tabriz, National Iranian Gas Company and Iranian nanotechnology initiative are gratefully acknowledged. The authors are grateful to Dr. Kavei for TEM images and Mr Bahrami for XRD patterns.

REFERENCES

[1] Y.Cheng, L.J.Wang, J.S.Li, Y.C.Yang, X.Y.Sun; Materials Letters, **59**, 3427-3430 **(2005)**.
[2] V.Rakic, V.Roc, V.Dondur, A.Auroux; Catalysis Today, **110**, 272-280 **(2005)**.
[3] S.Sang, F.Chang, Z.Liu, C.He, Y.He, L.Xu; Catalysis Today, **93**, 729-734 **(2004)**.
[4] R.T.Yang, A.Takahashi, F.H.Yang, A.J.Hernandez-Maldonado; Selective Sorbents for Desulfurization of Liquid Fuels.U.S.and Foreign Patent Applications, **(2002)**
[5] A.J.Hernández-Maldonado, R.T.Yang; Ind.Eng. Chem.Res., **42**, 123-128 **(2003)**.
[6] R.T.Yang, A.J.Hernández-Maldonado, F.H.Yang; Science, **301**, 79-84 **(2003)**.
[7] M.Khatamian, M.Dolatyari; Asian Journal of Chemistry, **19**, 5199-5210 **(2007)**.
[8] E.Erdem, N.Karapinar, R.Donat; Journal of Colloid and Interface Science, **208**, 309-314 **(2004)**.
[9] Y.Li, F.H.Yang, G.Qi, R.T.Yang; Catalysis Today, **116**, 512-518 **(2006)**.
[10] A.A.Ismail, R.M.Mohamed, O.A.Fouad, I.A.Ibrahim; Cryst.Res.Technol, **41**, 145-149 **(2006)**.
[11] G.Reading, T.Maurer, B.Kraushaar-Czarnetzki; Microporous and Mesoporous Materials, **57**, 83-92 **(2003)**.
[12] A.V.Ivanou, G.W.Graham, M.Shelef, Applied Catalysis B: Environmental, **21**, 243-258 **(1999)**.
[13] P.Dziekonski, W.A.Sokalski, E.Kassab, N.Ellavena; Chemical Physics Letters, **288**, 538-544 **(1998)**.
[14] M.A.Ali, B.Brisdon, W.J.Thomas; Applied Catalysis A: General, **252**, 149-162 **(2003)**.
[15] M.khatamian, M.Irani; Journal of the Iranian Chemical Society, **6**, 187-194 **(2009)**.
[16] M.M.J.Treacy, J.B.Higgins; Collection of Simulated XRD Powder Patterns for Zeolites, fourt revised ed., ELSEVIER, Amsterdam - London - New York - Oxford - Paris - Shannon – Tokyo, **(2001)**.
[17] D.J.Kim, H.S.Chung; Applied Clay Science, **24**, 69-

77 **(2003)**.

[18] L.O.Ohman, B.Ganemi, E.Bjornbom, K.Rahkamaa, R.L.Keiski, J.Paul; Materials Chemistry and Physics, **73**, 263-267 **(2002)**.

[19] J.C.Jensen, F.J.van der Gaag, H.V.Bekum; Zeolites, **4**, 369-376 **(1984)**.

[20] P.A.Jacobs, H.K.Beyer, J.Valyon; Zeolites, **1**, 161 **(1981)**.

[21] J.Aguado, D.P.Serrano, J.M.Escola, Rodriguez; Microporous and Mesoporous Materials, **75**, 41-49 **(2004)**.

[22] A.J.Hernández-Maldonado, F.H.Yang, G.Qi R.T.Yang; Applied Catalysis B: Environmental, **56**, 111-126 **(2005)**.

[23] C.F.Baes, R.E.Mesmer; The hydrolysis of cations, Wiley, New York, **(1976)**.

[24] A.J.Fowkes, R.M.Ibberson, M.J.Rosseinsky; Chem.Mater.,**14**, 590-596 **(2002)**.

[25] M.A.Keane; Microporous Mater,**4**, 356-364 **(1995)**.

[26] S.Velu, Xiaoliang Ma, Chunshan Song; Ind.Eng. Chem.Res.,**42,** 5293-5304 **(2003)**.

[27] T.F.Guidry, G.L.Price; J.Catal.,**181**, 16-23 **(1999)**.

[28] G.Turnes Palomino, P.Fisicaro, S.Bordiga, A.Zecchina, E.Giamello, C.Lamberti; J.Phys. Chem.B, **104**, 4064-4073 **(2000)**.

[29] F.X.Llabre'S.I.Xamena, P.Fisicaro, G.Berlier, A.Zecchina, G.Turnes Palomino, C.Prestipino, S.Bordiga, E.Giamello, C.Lamberti; J.Phys. Chem.B, **107**, 7036-7043 **(2003)**.